

Type I Interferon Signaling Protects Mice From Lethal Henipavirus Infection

Kévin P. Dhondt,^{1,2,3,a} Cyrille Mathieu,^{1,2,3,a} Marie Chalons,^{1,2,3} Joséphine M. Reynaud,^{1,2,3} Audrey Vallve,⁴ Hervé Raoul,⁴ and Branka Horvat^{1,2,3}

¹INSERM U758, Human Virology F-69365, France; ²Ecole Normale Supérieure de Lyon, Lyon, France; ³University of Lyon 1, Lyon Cedex 07 69365, France; and ⁴INSERM- Laboratoire P4 Jean Mérieux, Lyon 69365, France

Hendra virus (HeV) and Nipah virus (NiV) are closely related, recently emerged paramyxoviruses that form *Henipavirus* genus and are capable of causing considerable morbidity and mortality in a number of mammalian species, including humans. However, in contrast to many other species and despite expression of functional virus entry receptors, mice are resistant to henipavirus infection. We report here the susceptibility of mice deleted for the type I interferon receptor (IFNAR-KO) to both HeV and NiV. Intraperitoneally infected mice developed fatal encephalitis, with pathology and immunohistochemical features similar to what was found in humans. Viral RNA was found in the majority of analyzed organs, and sublethally infected animals developed virus-specific neutralizing antibodies. Altogether, these results reveal IFNAR-KO mice as a new small animal model to study HeV and NiV pathogenesis, prophylaxis, and treatment and suggest the critical role of type I interferon signaling in the control of henipavirus infection.

Keywords. Nipah virus; Hendra virus; type I interferon; animal model; encephalitis.

Within the past decade a number of new zoonotic viruses emerged from flying foxes to cause serious disease outbreaks in man and livestock. Hendra virus (HeV) came to light in 1994 as the causative agent of an acute respiratory disease in horses in Brisbane (Australia) with a fatal human case [1]. Naturally hosted by fruit bats (*Pteropus* species), HeV currently poses a serious threat to livestock in Australia, with sporadic lethal transmissions to humans. In 1998 in Malaysia, the closely related Nipah virus (NiV) was recognized as infecting pigs and subsequently humans, inducing encephalitis with 40% fatality [2]. Since then, and almost every year, outbreaks of NiV infection cause severe encephalitis in Bangladesh and India with a fatality case rate approaching 75% [3]. Multiple

rounds of person-to-person NiV transmission are observed [3, 4], thus further extending the risk of NiV infection in humans. In addition to acute infection, these viruses cause asymptomatic infections and may lead to late-onset or relapsing encephalitis years after initial infection [5]. Recently, 23 new distinct viral clades closely related to HeV and NiV have been identified in 6 bat species in 5 different African countries, thus widening significantly the geographic distribution of these viruses [6]. Although most closely related to *Morbillivirus*, a few distinctive properties of NiV and HeV, including their much larger genome size, led to their classification within the *Henipavirus* genus of the *Paramyxoviridae* family [7]. Because of their ability to infect humans with high pathogenicity, their wide host range and potent interspecies transmission, and the lack of an efficient treatment, the HeV and NiV were classified as biosecurity level 4 (BSL-4) pathogens.

Currently, very little is known about *Henipavirus* pathogenesis, and further studies depend largely on available animal models. Both HeV and NiV display an exceptionally broad host range. In addition to bats, which do not develop any apparent clinical disease, successful natural and experimental infection has been

Received 10 May 2012; accepted 31 July 2012; electronically published 22 October 2012.

^aThese authors contributed equally to this article.

Correspondence: Branka Horvat, MD, PhD, INSERM U758, 21 Ave Tony Garnier, 69365 Lyon, France (branka.horvat@inserm.fr).

The Journal of Infectious Diseases 2013;207:142–51

© The Author 2012. Published by Oxford University Press on behalf of the Infectious Diseases Society of America. All rights reserved. For Permissions, please e-mail: journals.permissions@oup.com.

DOI: 10.1093/infdis/jis653

observed in horses, cats, ferrets, pigs, guinea pigs [8], and monkeys [9–11], and the only small rodent model of henipavirus infection described so far is the Syrian golden hamster [12, 13]. Though the use of hamsters provided significant advances in *Henipavirus* research, this model suffers of major limitations due to the poor immunological and genetic toolbox that is currently available. Ephrin B2 and ephrin B3 proteins act as functional receptors for henipavirus and are highly conserved across vertebrate species including mice [14]; nevertheless, mice are known to be resistant to both NiV [12] and HeV infection [15].

Type I interferon (IFN-I) family consists of several subtypes, including 13 IFN- α isoforms, IFN- β , IFN- ϵ , IFN- κ , and IFN- ω . They all share widely expressed common cell surface receptor, composed of 2 chains, IFNAR1 and IFNAR2, capable of activating a complex intracellular signaling pathway, leading to the activation of numerous cellular genes and playing an important role in the control of viral infections [16]. IFN-I induces an antiviral state within cells through the upregulation and activation of antiviral proteins (eg, RNA-activated protein kinase, RNaseL, MxA) [17, 18] and by modulating adaptive immune responses [19]. To evaluate the role of IFN-I in resistance of mice to henipavirus infection, we analyzed susceptibility of mice lacking functional IFN-I receptor (IFNAR-KO mice) [20] to infection by NiV and HeV. Henipavirus infection in these animals induced development of fatal encephalitis with pathological lesions close to those observed in humans and surviving animals developed virus-neutralizing antibodies. Thus, IFNAR-KO mice represent a potent small animal model to study HeV and NiV pathogenesis, prophylaxis, immune response, and treatment. Furthermore, our data point to a critical role of IFN-I signaling in the control of henipavirus infection.

METHODS

Virus

HeV, obtained from Porton Down laboratory, UK, NiV (isolate UMMC1, GenBank AY029767) [21], and recombinant NiV-EGFP [22] were prepared by infecting Vero-E6 cells, in the INSERM Jean Mérioux BSL-4 laboratory in Lyon, France.

Preparation and Infection of Primary Brain Glial Cell Cultures

Glial cells were extracted by disruptions of cortex from brains of 2–3 day-old mice, and cultures were prepared as described elsewhere [23]. Briefly, cells were homogenized and plated in wells precoated with poly-D-lysine 50 $\mu\text{g}/\text{mL}$ in phosphate-buffered saline (PBS). Cells were cultured in 600 μL of medium (DMEM-glutamax [Gibco], 20% fetal calf serum, 0.5 mg/mL gentamycin, 10 mM HEPES) at 37°C in 5%CO₂, for 9–15 days and then infected with NiV. Production of infectious NiV in supernatant was followed by titration on Vero cells as described elsewhere [12].

Infection of Mice

Groups of 5–6 type I IFN Receptor Knock-Out (IFNAR-KO) mice [20] and wild-type C57BL/6 mice (PBES, ENS-Lyon, France) 4–12 weeks old (age homogenous within an experimental group) were anesthetized and infected either intraperitoneally with 0.4 mL of virus, intranasally with 30 μL of virus, or intracerebrally with 50 μL of virus or with equivalent volume of PBS (mock). Surviving animals were followed over 21 days after inoculation. All animals were handled in strict accordance with good animal practice and experiments were approved by Regional Ethical Committee CECCAPP.

Quantitative Reverse-Transcription Polymerase Chain Reaction (RT-qPCR)

RNA was extracted from primary glial cultures and organs (10–30 mg) of mock and henipavirus-infected mice as described elsewhere [24, 25]. Reverse transcription was performed on 0.5 μg of total RNA using the iScript cDNA synthesis kit (Bio-Rad) and run in Biometra T-GRADIENT PCR device, using NiV nucleoprotein (N)-specific and murine glyceraldehyde 3-phosphate dehydrogenase (GAPDH)-specific primers as described elsewhere [24, 25]. HeV N and IFN α 1, -2, -4, -5, -6, -7, -9, -11, -12, -13, and -14 and IFN β 1-specific primers were designed using Beacon 7.0 software, and validated for their efficacy close to 100%: HeV-N forward: GCCGGCTTCTTTGCGACTATC, HeV-N reverse: CGCTC GAGGCCCTATTTCTCTG, IFN- α forward: CTCTGTGCTT TCCTGATG, IFN- α reverse : CCTGAGGTTATGAGTCTGA, IFN- β forward : TCCACTTGAAGAGCTATTAC, and IFN- β reverse: CATTCTGAGGCATCAACT. Calculations were performed using the 2^{ΔΔCT} model, according to the MIQE guideline and normalized by the standard deviation of the average GAPDH expression, as described elsewhere [24, 25].

Histology and Immunohistochemistry (IHC)

Histology and IHC were performed as described elsewhere [25]. For conventional histology, slides were rapidly colored in modified Harris hematoxylin (Sigma–Aldrich) 1:3 in PBS and then washed. Eosin B-0.1% (Sigma–Aldrich) was used for counterstaining. Colored slides were dehydrated through graded alcohols and xylene. Sections were mounted with DPX mounting medium and cover-slipped. For IHC study a primary rabbit anti-NiV N purified antibody (ValBex, France) was applied diluted at 1:1000 in PBS with 1%, of bovine serum albumin overnight at 4°C. Further steps were performed as described elsewhere [25].

For immunofluorescence study, the same protocol as IHC was used with the additional step of permeabilization performed after antigen retrieval for 45 minutes in PBS plus 0.2% Triton X-100. A secondary goat anti-rabbit conjugated with Alexa Fluor 488 (Life Technologies) antibody was used at 1:400 for 1 hour at room temperature. After 2 washes in PBS,

NeuroTrace (Molecular Probes) 1:150 was applied for 20 minutes at room temperature. Slides were washed 10 minutes in PBS plus 0.1% Triton X-100, washed 3 times in PBS for 10 minutes, and mounted. Slides were analyzed with Zeiss LSM-710 fluorescence microscope equipped with Zeiss Zen software.

Virus Neutralization Assay

NiV and HeV neutralizing antibodies were assayed using serial 2-fold dilutions of serum, as described elsewhere [13]. Briefly, samples were incubated with virus (10–30 plaque-forming units [PFU] per well), and Vero cells (2.5×10^4) were added to each well and incubated for 5 days. Relative neutralizing titers are defined as the reciprocal dilution of serum samples that completely inhibited the cytopathic effect of either NiV or HeV.

Statistical Analysis

Data were expressed as mean and standard deviation (SD). Statistical analyses were performed using Mann–Whitney *U* test, 2-way analysis of variance (ANOVA) test followed with Bonferroni's post-test, χ^2 test (survival), and LD₅₀ was calculated using Spearman–Kärber test.

RESULTS

Nipah Virus Infects Primary Murine Brain Glial Cell Cultures

To determine the importance of Type I IFN in henipavirus infection, we first compared the permissiveness of primary glial brain cell cultures from wild-type mice with those obtained from IFNAR-KO mice to NiV infection (Figure 1). Although cultures from both murine lines were similarly susceptible to NiV-EGFP infection at high multiplicity of infection (MOI, 1 PFU/cell; Figure 1C–1H), cultures derived from IFNAR-KO mice produced significantly more infectious particles than cultures from wild-type mice, when infected with a low dose of NiV (0.02 PFU/cell; Figure 1H), without significant differences in cell viability during the first 48 hours postinfection. In cultures from both wild-type and IFNAR-KO mice NiV induced strong production of IFN β -specific messenger RNA (Figure 1I and 1J) at the similar level but not IFN α , which was detected only at the basal level (data not shown). These results suggested the importance of IFNAR signaling in the protection of primary brain cells from the infection with low doses of NiV, thus encouraging further *in vivo* experiments with this murine model.

Henipavirus-Induced Clinical Signs in Mice

We next compared the susceptibility of wild-type and IFNAR-KO mice to NiV infection, using different routes of inoculation. As reported elsewhere [12], wild-type mice were completely resistant to intraperitoneal infection (Figure 2A).

However, they were highly susceptible when NiV was injected intracerebrally with 10^5 PFU, and all mice died within the first 6 days. In contrast, IFNAR-KO mice showed high susceptibility to NiV infection whatever the route of administration (Figure 2B). While all intracerebrally and intraperitoneally inoculated IFNAR-KO mice succumbed to infection, intranasal route was lethal in 3 of 5 mice. In accord to the higher susceptibility of IFNAR-KO brain cultures to low dose infection with NiV (Figure 1H), IFNAR-KO mice were also more susceptible to intracerebral infection than wild-type mice as shown by 2 days earlier lethality in all mice ($P = .0237$, χ^2 Chi test).

IFNAR-KO mice infected intraperitoneally showed different clinical signs from behavioral troubles to neurological disabilities. The weight loss (from 15% to 25%) was regularly observed 1–2 days before death and was thus a good predictive marker of lethal outcome. In the early stages of infection, sickness of IFNAR-KO mice led to behavioral troubles with agitation, edginess, or a lack of grooming. When the disease progressed, signs of pain associated with neurological disabilities appeared. Mice presented a painful face (orbital tightening, nose bulge, and ears and whiskers drawn back position) as referred in the mouse grimace scale [26], lordosis, aggressiveness, and prostration. At late stages of infection, the neurological symptoms regularly worsened with locomotor disabilities, tilted head, or paralysis.

IFNAR-KO mice were also susceptible to HeV infection; however, this virus exhibited a somewhat lower pathogenicity than NiV (Figure 2C). Although 4-week-old IFNAR-KO mice all succumbed to intraperitoneal HeV infection, the susceptibility decreased gradually with age, and in 11-week-old mice HeV infection induced only 50% mortality. Moreover, and in contrast to NiV infection, IFNAR-KO mice were resistant to intranasal infection by HeV.

The survival of groups of 5 IFNAR-KO mice infected intraperitoneally with increasing doses of NiV from 100 to 10^6 PFU (Figure 2D) was monitored. All animals that received the highest dose died between days 6 and 9. No fatality was recorded beyond 10 days postinfection in any groups, and one mouse having received 10^4 PFU recovered after a long convalescence period. This allowed calculation of the NiV lethal dose at which 50% of animal succumbed to the intraperitoneal infection (LD₅₀) to be 8×10^3 PFU in IFNAR-KO mice (Figure 2D).

Spread of Henipavirus Infection Within Infected Mice

Virus spreading to different murine organs was analyzed by quantifying the expression of nucleoprotein (N) RNA by RT-qPCR (Figure 3). The N expression was found in all analyzed organs of HeV intraperitoneally infected IFNAR-KO mice. However, the RNA levels in HeV intranasally infected mice were statistically lower in all organs ($P < .005$), compared to

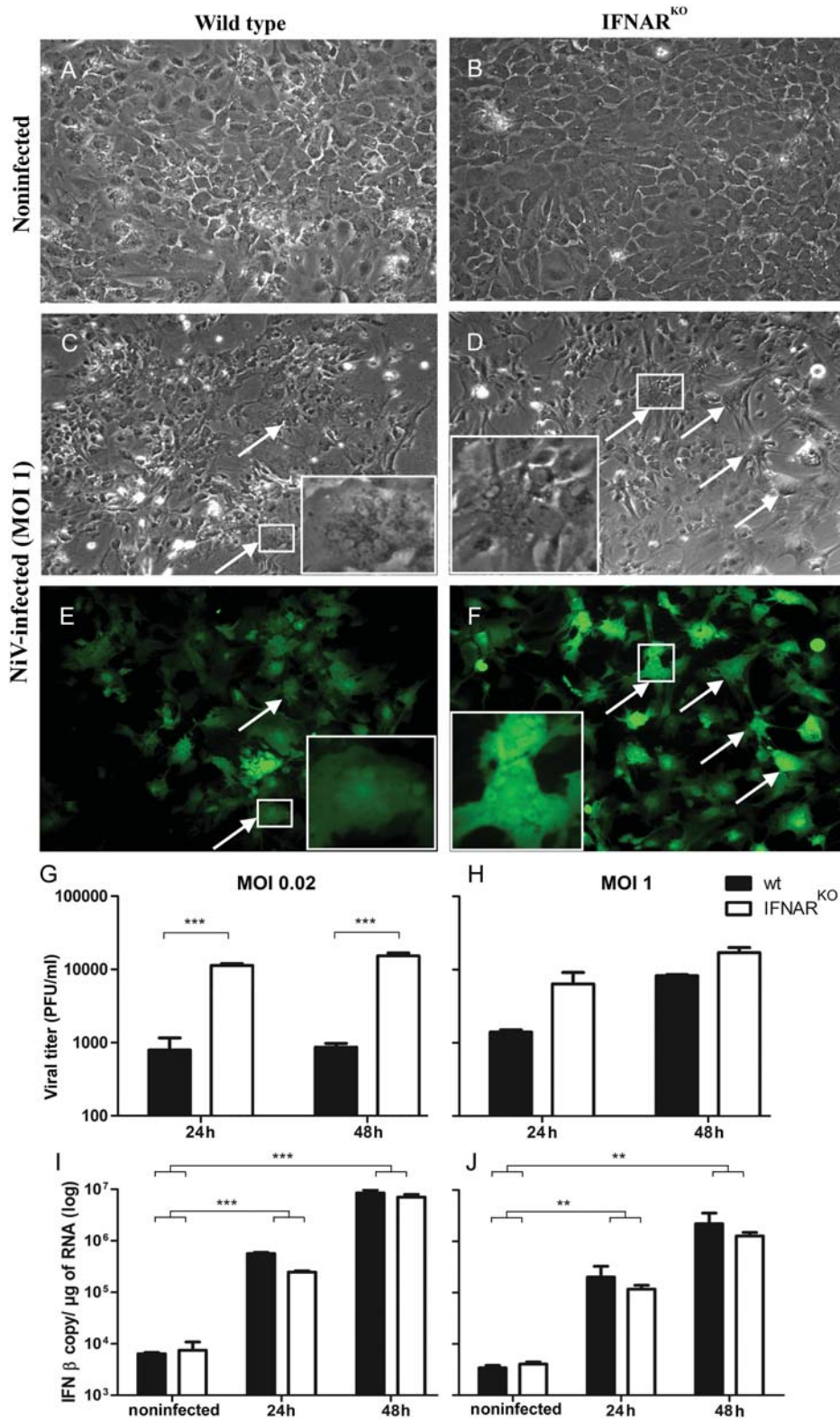


Figure 1. Permissiveness of primary murine brain glial cell cultures to NiV infection. Brain cultures from either wild-type (A, C, E) or IFNAR-KO mice (B, D, F) were mock-infected (A and B), or infected with NiV-EGFP (MOI=1) and observed 48 h later under light (A–D) and fluorescent (E and F) microscope (×100). Formation of large multinuclear syncytia is indicated by arrows and presented in insert at higher (×300) magnification (C–F). Supernatants (G and H) and cells (I and J) from cultures obtained after NiV infection at MOI=0.02 (G and I) or MOI=1 (H and J) were taken at 24 and 48 h postinfection and titrated on Vero cells (G and H), and RNA was analyzed by RT-qPCR for the expression of IFN- β (I and J). Results are presented as average viral titers from triplicate cultures \pm SD (G and H; * P <.01, Mann–Whitney U test) or no. of copies/ μ g of IFN β -specific RNA \pm SD (I and J, ** P <.01, *** P <.001; 2-way ANOVA test followed with Bonferroni post-test).

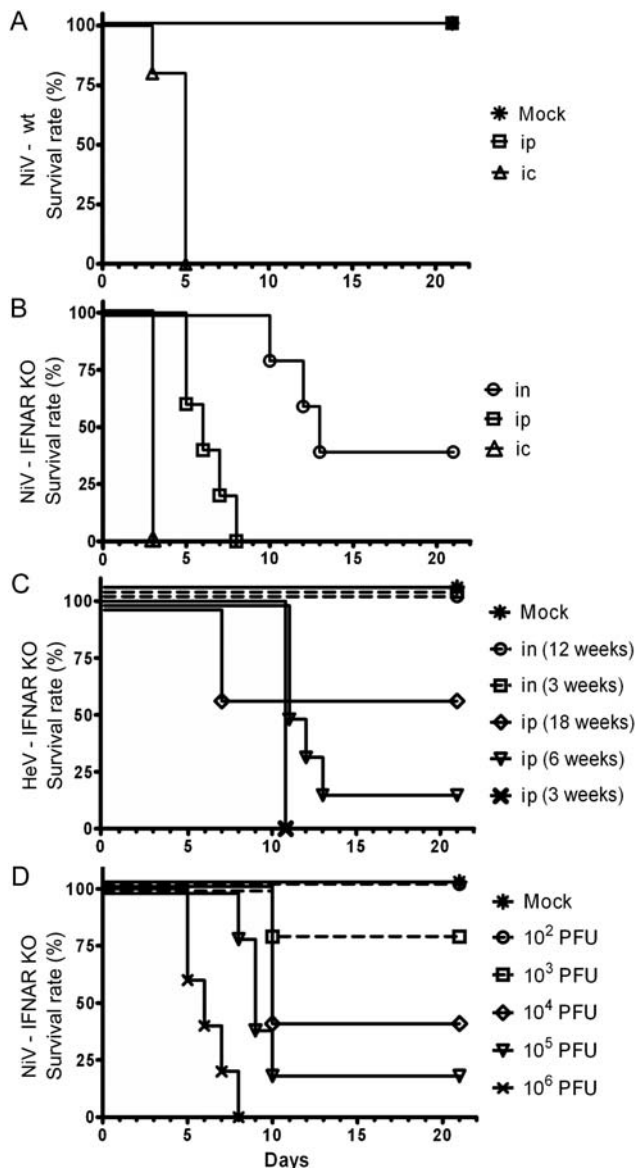


Figure 2. Survival of mice infected by henipavirus. C57BL/6 wt (A) and IFNAR-KO (B–D) mice were infected with either NiV (A, B, D) or HeV (C). Intraperitoneal (ip; A–D) and intranasal (in; B and C) infections were performed with 10⁶ PFU and intracerebral (ic) infections (A, B) with 10⁵ PFU of virus. (D) LD₅₀ was established in 9–10-week-old IFNAR-KO mice using increasing doses of NiV from 10² to 10⁶ PFU injected intraperitoneally. Animals were monitored daily for the development of clinical symptoms over 3 weeks.

intraperitoneally infected mice (Figure 3A). This correlated with the survival of all mice infected intranasally with HeV (Figure 2C), suggesting that intranasal inoculation of HeV results in systemic infection but at lower level than intraperitoneal infection route. Expression of NiV N followed the similar pattern as HeV N expression in intraperitoneally infected mice (Figure 3B), with apparently higher level of NiV-N expression in lungs of NiV-infected IFNAR-KO mice than in

intraperitoneal HeV-infected mice, in accord to higher susceptibility of these mice to intranasal infection (Figure 2B and 2C). In contrast to IFNAR-KO mice, C57BL/6 mice showed only very low level of RNA copies of NiV-N in the lung (2 samples) and in the spleen (1 sample) and were under detection level in the other organs. Moreover, some NiV-N RNA was detected in surviving animals, although at 100- to 1000-fold lower level than in mice succumbing to the infection.

Histopathological Studies of Henipavirus-Infected Mice

Upon necropsy, NiV- and HeV-infected IFNAR-KO mice exhibited congestion with scattered small hemorrhagic lesions in the brain and heart. In NiV-infected animals, focal necrosis and petechial hemorrhages were observed in the liver and kidney. No particular lesions of liver and kidney were noticed in HeV-infected animals. Less frequently, congestion of the lungs and edema of the bladder wall were also observed. Upon histological and immunohistological analysis of organs from infected IFNAR-KO mice, both viruses appeared to affect the brain, causing parenchymal and meningeal nonsuppurative inflammation, the former being predominant after HeV infection. Vascular lesions were numerous and included wide-spread vasculitis, often associated with hemorrhages (Figure 4D), leukocyte infiltration, and perivascular cuffing (Figure 4G). Neurons close to sites of vasculitis and meningitis lesions showed eosinophilic inclusions, suggesting a hypoxic-ischemic state in the brain (Figure 4G). IHC analysis of the brain from both NiV- and HeV-infected IFNAR-KO mice revealed infected ependymal cells (Figure 4L) and neuron-shaped cells (Figure 4J), which was further confirmed by immunofluorescence (Figure 5). Histopathology of lungs revealed intense inflammation with edema, focal necrotizing alveolitis (Figure 4E), and vasculitis (Figure 4H). IHC indicated the presence of NiV antigen in different cell types, including pneumocytes (Figure 4K) and cells from the pseudostratified epithelium. Hepatic lesions observed in NiV-infected animals were severe, with signs of acute and intense hepatitis. Focal necrosis, as well as vasculitis, large syncytia, hemorrhages, and inflammation were abundant (Figure 4F). In HeV-infected animals, hepatic lesions were not significant (Figure 4I). Histopathology of the kidney showed moderate inflammation associated with light vasculitis (data not shown). In contrast to IFNAR-KO mice, the histopathological findings in C57BL/6 were poor, with only occasionally noticed very mild inflammation of the brain (2 out of 6 analyzed samples, data not shown). Furthermore, no viral protein could be detected by IHC.

Neutralizing Antibody Response

Infected mice were then analyzed for their capacity to produce virus-specific neutralizing antibodies in the serum. Animals that succumbed to henipavirus infection within the first 7 days postinfection did not generate neutralizing antibodies

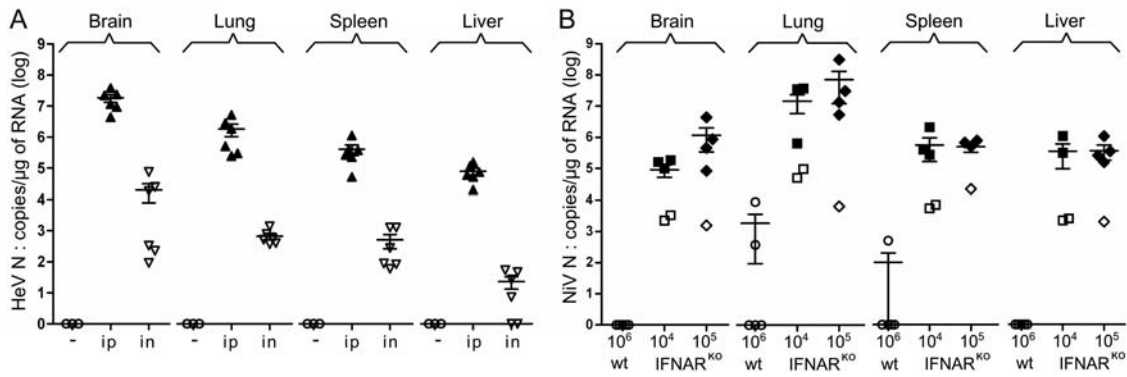


Figure 3. Analysis of henipavirus replication in different murine organs by RT-qPCR. (A) 4-week-old IFNAR-KO mice were inoculated either intranasally (in) or intraperitoneally (ip) with 10^6 PFU of HeV. (B) IFNAR-KO and C57Bl/6 mice were infected intraperitoneally with indicated doses of NiV. Organ samples were analyzed for the expression of either HeV (A) or NiV N gene (B) by RT-qPCR, either from mice succumbing to the infection (5–10 days postinfection) or mice surviving infection at the end of experiment (21 days postinfection). Results are expressed in no. of copies/ μ g of RNA extracted from organs collected at necropsy, and horizontal lines correspond to the average of each group. Open symbols represent animals that survived to the infection and were analysed 21 days postinfection, and filled symbols represent those that succumbed to the infection. All RT-qPCR experiments were performed in duplicates. The difference between the 2 routes of HeV infection was established statistically for all tested organs ($P < .005$, Mann-Whitney *U* test).

(data not shown). However, surviving IFNAR-KO mice, infected with HeV by both intraperitoneal and intranasal routes, developed seroneutralizing antibodies 3 weeks postinfection (Figure 6A). In correlation to their higher susceptibility to HeV infection, younger mice (4 weeks old) developed significantly higher titer of neutralizing Abs compared to 12-week-old IFNAR-KO intranasally infected mice ($P = .0263$). Production of neutralizing Abs in intranasally NiV-infected mice was also rather low (Figure 6B). In wild-type C57BL/6 mice, only 2 of 5 NiV-infected animals developed a very low level of neutralizing antibodies (Figure 6B). In contrast, IFNAR-KO infected intraperitoneally with a sublethal NiV inoculum developed high titer of seroneutralizing antibodies, similarly to intraperitoneally HeV-infected animals, thus showing the capacity of IFNAR-KO mice to efficiently produce humoral immune response against henipavirus within the first 3 weeks of infection.

DISCUSSION

This study analyzes the role of type I IFN system in henipavirus pathogenesis and demonstrates the critical role of IFNAR signaling in the protection of mice from lethal HeV and NiV infection. IFN-I can exert antiviral effects at multiple levels, causing the induction of antiviral genes as well as augmentation of antigen-presenting cell and lymphocyte functions. IFN-I may affect the survival of diverse cell populations: it could prolong neuron and astrocyte survival following growth factor deprivation or serum starvation [27, 28]. It has been hypothesized that the ability of IFNs to inhibit cell death may preserve neuronal populations and limit disease in the central

nervous system (CNS) induced by either viral infection or inflammation [29]. The selective increased permissiveness of primary brain glial cultures lacking IFNAR signaling after infection with NiV at low but not high MOI strongly suggests that mouse cells can efficiently detect NiV infection and secrete IFN-I to protect surrounding cells from virus spreading, although NiV-induced production of IFN-I by neuronal cells may be limited [30]. Only a small population of infected neurons produces IFN-I following infection with certain viruses, and IFN-I was shown to be principally made by parenchymal cells in the brain [31]. Our results have demonstrated the critical importance of IFNAR signaling for the protection of mice from henipavirus infection in vivo. In addition to the local protection of brain cells from infection, it is also possible that systemic transmission of the virus, retrograde axonal transport, and neuroinvasion are more efficient in the absence of the functional IFN-I system, as shown for poliovirus [32], and could thus contribute to the higher susceptibility of IFNAR-KO mice to henipavirus infection. Altogether, these results are consistent with infection of IFNAR-KO mice with other neurotropic RNA viruses, including vesicular stomatitis virus [20], measles [33], coronavirus [34], or West Nile virus infection [35], in which the absence of IFNAR downstream signaling highly increases the susceptibility to infection.

Henipavirus infects a large spectrum of mammalian species (hamsters, pigs, dogs, horses ...), but mice are resistant to infection although they do express functional cell entry receptor for henipavirus, ephrin B2, and ephrin B3 molecules [14]. HeV and NiV encode several proteins that block IFN-I in different cell types and thus counteract innate immune response

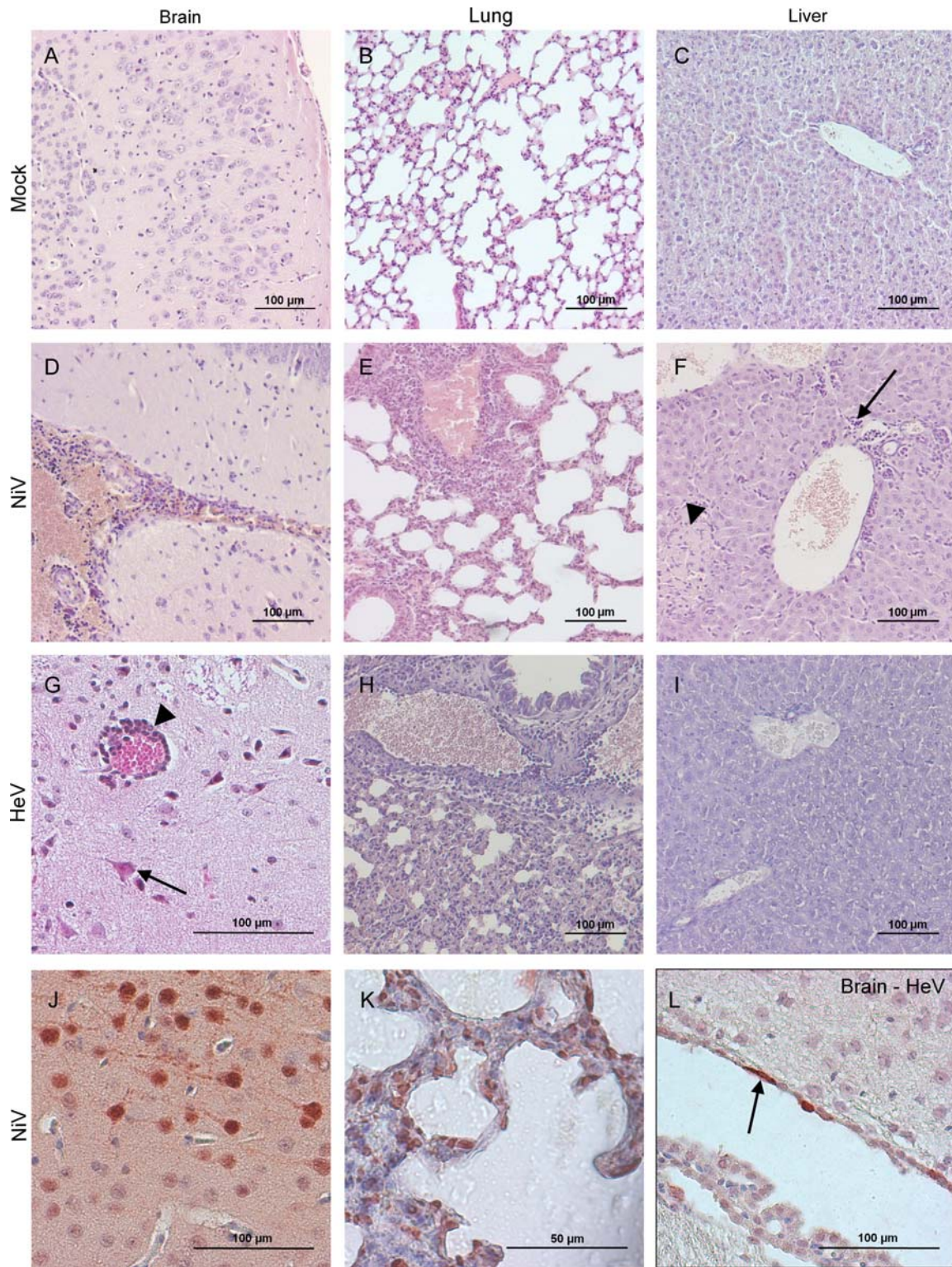


Figure 4. Pathology of henipavirus infection in IFNAR-KO mice. Animals were inoculated intraperitoneally with either mock preparation (A–C), or 10^6 PFU of either NiV (D–F, J and K) or HeV (G–I, L). Brain (A, D, G, J, L), lungs (B, E, H, K), or liver (C, F, I) were analyzed after hematoxylin and eosin staining (A–I) or by immunohistochemistry (J–L) 5–7 days postinfection. (D) Severe vasculitis, hemorrhage, and leukocyte infiltration in NiV-infected brain. (G) Perivascular cuffing (arrow head) and eosinophilic neurons (arrow) following HeV infection. (J) Staining of NiV antigens in neurons. (L) Staining of HeV antigens in brain ependymal cells (arrow). Vasculitis, alveolar necrosis and inflammation following either NiV (E) or HeV infection (H). (K) Staining of NiV antigens in pneumocytes. (F) Severe hepatitis lesions, leukocytes infiltration (arrow) and necrotizing plaques (arrow head) in NiV-infected mouse. (I) No significant lesions were observed in the liver of HeV-infected animal.

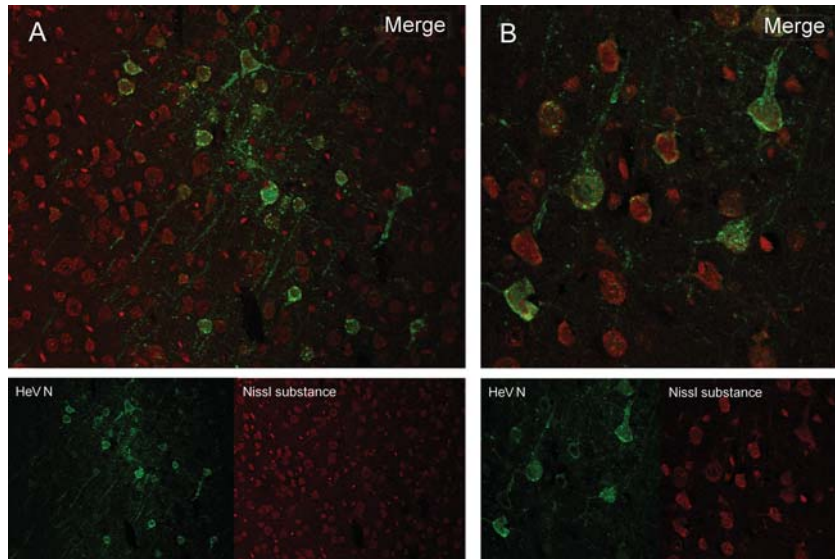


Figure 5. HeV infection in neurons of IFNAR-KO mice. Animals were inoculated intraperitoneally with 10^6 PFU of HeV. Brains were analyzed by immunofluorescence at 6 days postinfection and stained with a rabbit polyclonal anti-NiV N antibody (*green*) and NeuroTrace, specific for neuronal Nissl substance (*red*). (A) Axonal labeling of HeV-infected neurons. Magnification $\times 20$. (B) Typical viral inclusions in the cytoplasm of infected neurons. Magnification $\times 63$.

[36], and resistance to henipavirus infection in mice may be linked to inability of viral proteins to interact with their homologous murine molecular partner. Understanding the underlying mechanism, by which henipavirus infection is so efficiently controlled in mice, may help the development of more effective countermeasures in humans. Furthermore, the critical role of IFN-I signaling in control of the HeV and NiV infection observed in this study, and recent observations that in human cell lines NiV and HeV inhibit IFN-I production rather than IFN-I signaling pathways [37], as well as previous finding that interferon inducer poly(I)-poly(C(12)U) could prevent Nipah virus-induced mortality [38], suggest a potential for IFN-I treatment as a possible postexposure therapeutic.

Both NiV and HeV are disseminated rapidly to different organs of IFNAR-KO mice, following intraperitoneal infection and are transmitted to the brain, where they induce lethal encephalitis. Similarly to henipavirus infection in human [39, 40], infected mice developed neurological signs and CNS pathology, with parenchymal brain cell infection, meningitis, and vasculitis-induced microinfarctions, most probably responsible for the lethal outcome of the disease. Histopathological studies in different organs revealed the presence of widespread vasculitis, hemorrhages, and strong inflammation. Thus, these results emphasize number of similarities between this new IFNAR-KO mouse model and the well-established hamster model [12, 13], although the LD_{50} was much higher in mice

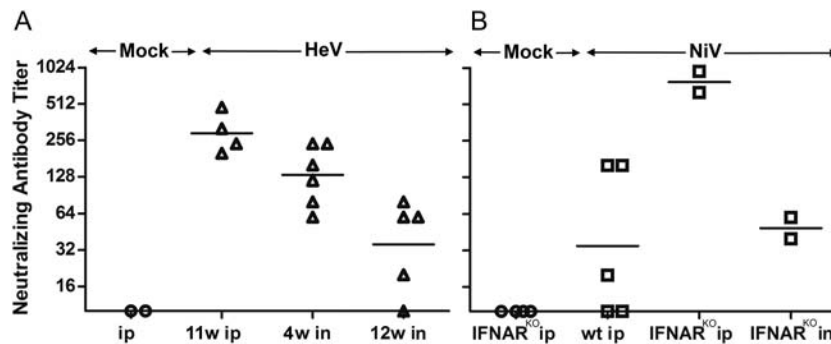


Figure 6. Production of neutralizing antibodies in mice surviving henipavirus infection. Mice were infected with 10^6 PFU of either HeV (A) or NiV-specific (B) and virus-specific neutralizing antibodies were assessed in the serum at 21 days postinfection. Horizontal lines correspond to the average titer in each group. HeV-infected mice were 4, 11 and 12 weeks-old in indicated groups (4 w, 11 w, and 12 w) and NiV-infected mice were either 4 weeks old (intranasal [in]) or 10 weeks old (intraperitoneal [ip]).

than in hamsters, suggesting that they may differ from hamsters in some additional factor(s) important for henipavirus infection. Previous work suggested that infection of hamsters with a high dose of NiV or HeV resulted in acute respiratory distress, whereas low doses induced the development of neurological signs and more systemic spread of the virus [41]. In agreement to their lower susceptibility, development of mainly neurological disease in this murine model suggests that the infection of IFNAR-KO mice with henipavirus mimics the low-dose infection of hamsters. Furthermore, as shown in hamsters [12], IFNAR-KO mice were more susceptible to intraperitoneal than to intranasal NiV infection. In the latter route of inoculation, they displayed the progression of neuronal signs, along with breath difficulties in 60% of infected animals, followed by delayed mortality compared to intraperitoneally infected mice. Finally, and in compliance with the hamster model [13], we have observed the age-related susceptibility to intraperitoneal HeV infection in mice, which declines with older age of animals. Curiously, IFNAR-KO mice were not susceptible to HeV by the intranasal route. Significantly lower level of HeV N was detected in different organs of intranasally infected mice, compared to intraperitoneally infected mice, indicating that some virus replication did take place but was probably insufficient to lead to mortality. These results may reflect some differential permissiveness of the murine respiratory system to initial stages of NiV and HeV replication, possibly related to distribution and/or different binding affinity for the entry receptors [14]. Likewise, in hamster model NiV initially replicates in the upper respiratory tract epithelium, whereas HeV initiates infection in the interstitium of the lungs and not in the trachea or bronchi [41].

Although IFNAR-KO mice show certain differences in immune response compared to wild-type mice, due to the lack of IFN-I signaling [42], they could efficiently mount both humoral and cellular immune response and have been already used in the evaluation of different vaccine strategies, including vaccination against Dengue virus, SARS virus, and West Nile virus [43–45]. Since henipavirus infection elicits production of high levels of neutralizing antibodies in IFNAR-KO mice, these animals thus constitute a useful model to evaluate vaccination strategies against henipavirus. Furthermore and as opposed to other characterized models, this new murine model provides access to the numerous and powerful tools available for mice, which should be of critical help for in-depth immunobiological and genetic studies of henipavirus infection and could substantially promote the discovery of new therapeutic and prophylactic targets as well as the assessment of drug candidates and vaccines.

Notes

Acknowledgments. Authors thank S. Mely, F. Jacquot, A. Duthey, D. Cornec, and other biosafety team members from INSERM BSL4 “Jean

Mérieux” for their assistance, Professor K. T. Wong (Malaya University), Dr D. Gerlier, J. Welsch, and members of the INSERM-U758 group “Immunobiology of viral infections” for their help in the achievement of this study.

Financial Support. This work was supported by Institut National de la Santé et de la Recherche Médicale (INSERM) and Agence Nationale de la Recherche, K. D. was supported by Direction Générale de l’Armement (DGA) and INSERM.

Potential conflicts of interest. All authors: No reported conflicts.

All authors have submitted the ICMJE Form for Disclosure of Potential Conflicts of Interest. Conflicts that the editors consider relevant to the content of the manuscript have been disclosed.

References

- Murray K, Selleck P, Hooper P, et al. A morbillivirus that caused fatal disease in horses and humans. *Science* **1995**; 268:94–7.
- Chua KB, Bellini WJ, Rota PA, et al. Nipah virus: a recently emergent deadly paramyxovirus. *Science* **2000**; 288:1432–5.
- Lo MK, Rota PA. The emergence of Nipah virus, a highly pathogenic paramyxovirus. *J Clin Virol* **2008**; 43:396–400.
- Luby PS, Hossain MJ, Gurley ES, et al. Recurrent zoonotic transmission of Nipah virus into humans, Bangladesh, 2001–2007. *Emerg Infect Dis* **2009**; 15:1229–1233.
- Tan CT, Goh KJ, Wong KT, et al. Relapsed and late-onset Nipah encephalitis. *Ann Neurol* **2002**; 51:703–8.
- Drexler JF, Corman VM, Muller MA, et al. Bats host major mammalian paramyxoviruses. *Nat Commun* **2012**; 3:796.
- Wang LF, Yu M, Hansson E, et al. The exceptionally large genome of Hendra virus: support for creation of a new genus within the family *Paramyxoviridae*. *J Virol* **2000**; 74:9972–9.
- Weingartl HM, Berhane Y, Czud M. Animal models of henipavirus infection: a review. *Vet J* **2009**; 181:211–20.
- Marianneau P. Experimental infection of squirrel monkeys with Nipah virus. *Emerg Infect Dis* **2010**; 16:507–10.
- Geisbert TW, Daddario-DiCaprio KM, Hickey AC, et al. Development of an acute and highly pathogenic nonhuman primate model of Nipah virus infection. *PLoS ONE* **2010**; 5:e10690.
- Rockx B, Bossart KN, Feldmann F, et al. A novel model of lethal Hendra virus infection in African green monkeys and the effectiveness of ribavirin treatment. *J Virol* **2010**; 84:9831–9.
- Wong KT, Grosjean I, Brisson C, et al. A golden hamster model for human acute Nipah virus infection. *Am J Pathol* **2003**; 163:2127–37.
- Guillaume V, Wong KT, Looi RY, et al. Acute Hendra virus infection: analysis of the pathogenesis and passive antibody protection in the hamster model. *Virology* **2009**; 387:459–65.
- Bossart K. Functional studies of host-specific ephrin-B ligands as henipavirus receptors. *Virology* **2008**; 372:357–71.
- Westbury H, Hooper PT, Selleck PW, Murray PK. Morbilliviruses pneumonia: susceptibility of laboratory animals to the virus. *Aust Vet J* **1995**; 72:278–9.
- de Weerd NA, Samarajiwa SA, Hertzog PJ. Type I interferon receptors: biochemistry and biological functions. *J Biol Chem* **2007**; 282:20053–7.
- Sadler AJ, Williams BR. Interferon-inducible antiviral effectors. *Nat Rev Immunol* **2008**; 8:559–68.
- Gerlier D, Lyles DS. Interplay between innate immunity and negative-strand RNA viruses: towards a rational model. *Microbiol Mol Biol Rev* **2011**; 75:468–90, second page of table of contents.
- Stetson DB, Medzhitov R. Type I interferons in host defense. *Immunity* **2006**; 25:373–81.
- Muller U, Steinhoff U, Reis LF, et al. Functional role of type I and type II interferons in antiviral defense. *Science* **1994**; 264:1918–21.
- Chan YP, Chua KB, Koh CL, Lim ME, Lam SK. Complete nucleotide sequences of Nipah virus isolates from Malaysia. *J Gen Virol* **2001**; 82:2151–5.

22. Yoneda M, Guillaume V, Ikeda F, et al. Establishment of a Nipah virus rescue system. *Proc Natl Acad Sci U S A* **2006**; 103:16508–13.
23. Marignier R, Nicolle A, Watrin C, et al. Oligodendrocytes are damaged by neuromyelitis optica immunoglobulin G via astrocyte injury. *Brain* **2010**; 133:2578–91.
24. Mathieu C, Pohl C, Szecsi J, et al. Nipah virus uses leukocytes for efficient dissemination within a host. *J Virol* **2011**; 85:7863–71.
25. Mathieu C, Guillaume V, Sabine A, et al. Lethal Nipah virus infection induces rapid overexpression of CXCL10. *PLoS ONE* **2012**; 7:e32157.
26. Langford DJ, Bailey AL, Chanda ML, et al. Coding of facial expressions of pain in the laboratory mouse. *Nat Meth* **2010**; 7:447–9.
27. Barca O, Ferre S, Seoane M, et al. Interferon beta promotes survival in primary astrocytes through phosphatidylinositol 3-kinase. *J Neuroimmunol* **2003**; 139:155–9.
28. Chang JY, Martin DP, Johnson EM Jr. Interferon suppresses sympathetic neuronal cell death caused by nerve growth factor deprivation. *J Neurochem* **1990**; 55:436–45.
29. Yang CH, Murti A, Pfeffer SR, Basu L, Kim JG, Pfeffer LM. IFN α / β promotes cell survival by activating NF-kappa B. *Proc Natl Acad Sci U S A* **2000**; 97:13631–6.
30. Lo MK, Miller D, Aljofan M, et al. Characterization of the antiviral and inflammatory responses against Nipah virus in endothelial cells and neurons. *Virology* **2010**; 404:78–88.
31. Delhaye S, Paul S, Blakqori G, et al. Neurons produce type I interferon during viral encephalitis. *Proc Natl Acad Sci U S A* **2006**; 103:7835–40.
32. Lancaster KZ, Pfeiffer JK. Limited trafficking of a neurotropic virus through inefficient retrograde axonal transport and the type I interferon response. *PLoS Pathogens* **2010**; 6:e1000791.
33. Mrkic B, Pavlovic J, Rulicke T, et al. Measles virus spread and pathogenesis in genetically modified mice. *J Virol* **1998**; 72:7420–7.
34. Ireland DD, Stohlman SA, Hinton DR, Atkinson R, Bergmann CC. Type I interferons are essential in controlling neurotropic coronavirus infection irrespective of functional CD8 T cells. *J Virol* **2008**; 82:300–10.
35. Samuel MA, Diamond MS. Alpha/beta interferon protects against lethal West Nile virus infection by restricting cellular tropism and enhancing neuronal survival. *J Virol* **2005**; 79:13350–61.
36. Basler CF. Nipah and Hendra virus interactions with the innate immune system. *Curr Top Microbiol Immunol* **2012**; 359:123–52.
37. Virtue ER, Marsh GA, Wang LF. Interferon signaling remains functional during henipavirus infection of human cell lines. *J Virol* **2011**; 85:4031–4.
38. Georges-Courbot MC, Contamin H, Faure C, et al. Poly(I)-poly (C12U) but not ribavirin prevents death in a hamster model of Nipah virus infection. *Antimicrob Agents Chemother* **2006**; 50:1768–72.
39. Wong KT, Robertson T, Ong BB, et al. Human Hendra virus infection causes acute and relapsing encephalitis. *Neuropathol Appl Neurobiol* **2009**; 35:296–305.
40. Wong KT, Shieh WJ, Kumar S, et al. Nipah virus infection: pathology and pathogenesis of an emerging paramyxoviral zoonosis. *Am J Pathol* **2002**; 161:2153–67.
41. Rockx B, Brining D, Kramer J, et al. Clinical outcome of henipavirus infection in hamsters is determined by the route and dose of infection. *J Virol* **2011**; 85:7658–71.
42. Gough DJ, Messina NL, Clarke CJ, Johnstone RW, Levy DE. Constitutive type I interferon modulates homeostatic balance through tonic signaling. *Immunity* **2012**; 36:166–74.
43. Brandler S, Lucas-Hourani M, Moris A, et al. Pediatric measles vaccine expressing a dengue antigen induces durable serotype-specific neutralizing antibodies to dengue virus. *PLoS Negl Trop Dis* **2007**; 1:e96.
44. Despres P, Combredet C, Frenkiel MP, Lorin C, Brahic M, Tangy F. Live measles vaccine expressing the secreted form of the West Nile virus envelope glycoprotein protects against West Nile virus encephalitis. *J Infect Dis* **2005**; 191:207–14.
45. Liniger M, Zuniga A, Tamin A, et al. Induction of neutralizing antibodies and cellular immune responses against SARS coronavirus by recombinant measles viruses. *Vaccine* **2008**; 26:2164–74.